ORIGINAL PAPER

Synthesis and studies of homopolyamides based on 2,4-bis-(6-chlorocarbonyl-2-naphthyloxy)-6-(4-methyl-1-piperazinyl)-*s*-triazine

Shahrukh T. Asundaria · Hemant S. Patel · Keshav C. Patel

Abstract Ten homopolyamides have been synthesized by polycondensation of the monomer 2,4-bis(6-chlorocarbonyl-2-naphthyloxy)-6-(4-methyl-1-piperazinyl)-*s*-triazine and different diamines such as 4,4′-biphenyldiamine, 4,4′-diaminobenzanilide, 4,4′-diaminodiphenylmethane, 4,4′-diaminodiphenyl sulfone, 4,4′-diaminodiphenyl sulfonamide, 2,4-diaminotoluene, *o*-phenylenediamine, *m*-phenylenediamine, *p*-phenylenediamine, and ethylenediamine. All polyamides were characterized by solubility, density, viscosity measurements, IR, NMR spectroscopy, and thermogravimetric analysis. The products were found to possess high thermal stability.

Keywords Polycondensation · NMR spectroscopy · IR spectroscopy · Density · Viscosity

Introduction

A literature survey of the polymers containing an *s*-triazine moiety in their backbone reveals that these polymers are unique in the sense that they exhibit an unusual combination of the properties viz. high softening temperature, high glass transition point, and thermal stability along with fair processibility [1–5]. Historically and commercially, polyamides occupy an important place in the world of polymers. Carothers [6–9] first recognized that polymeric amides were formed by the reactions of diamines with dibasic acids. Aromatic polyamides are well-known high-performance polymeric materials for their excellent mechanical properties and good thermal stability. Aromatic polyamides are heat resistant polymers that generally exhibit outstanding mechanical properties and excellent thermal and oxidative stability [10, 11]. Because of these properties they are of major commercial and industrial importance [12, 13]. Because of chain stiffness and intermolecular hydrogen bonding between amide groups, wholly aromatic polyamides [14] are well known for high performance polymeric properties as they possess high melting points, good thermal stability, and excellent mechanical properties. Some of the main uses of polyamides or nylons are for synthetic fibres for the tire, carpet, stocking, and upholstery industries [14–16]. Use of polyamides as molding and extrusion resins for the plastics industry is also of increasing importance [17]. This has become possible only because of the particular characteristics of polyamide and availability of polyamides of varied structures. Reviewing the literature [18–20] one can conclude that aromatic polyamides are one of the important high-performance polymers which can be used in applications that demand service at enhanced temperatures, while maintaining their structure integrity and an excellent combination of chemical, physical, and mechanical properties.

Salunkhe et al. [21] reported a series of aromatic polyamides containing an *s*-triazine ring with thiophenoxy bonds synthesized by using Yamazaki's phosphorylation reaction. The polyamides were obtained in high yields. All polyamides were readily soluble in different solvents. Thermogravimetric analysis of the polyamides indicated no weight loss below 345 °C under a nitrogen atmosphere. Sagar et al. [22, 23] reported the synthesis of polyamides containing *s*-triazine rings (Fig. 1) by interfacial polycondensation. The polyamides were readily soluble at room temperature in polar solvents. Transparent, tough, and

S. T. Asundaria · H. S. Patel · K. C. Patel (✉)
Department of Chemistry, Veer Narmad South Gujarat University, Udhna-Magdalla Road, Surat 395007, India
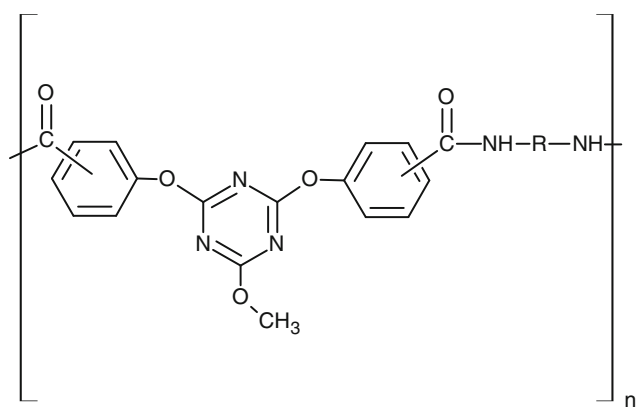e-mail: drkeshavpatel@rediffmail.com

Fig. 1 Polyamides containing *s*-triazine *rings*

flexible films could be cast from DMAc solution. TGA analysis of the polyamides indicated no weight loss below 350 °C under nitrogen atmosphere.

In the light of these facts, it would be significant and useful to synthesize new polyamides and to investigate their physical, spectral, and thermal properties. These novel polyamides are promising as materials of high thermal stability and processibility.

The aim of the present work is to explore experimental conditions for the synthesis of polymers and hence to select optimum reaction conditions and to investigate the effect of chemical structure of the diamines on polymers.

In our laboratory, we have synthesized and characterized various polyamides and copolyamides based on 2,4-bis(2-chlorocarbonyl-1-naphthyloxy)-6-(1-piperidinyl)-*s*-triazine [24], 2,4-bis[2-(chlorocarbonyl)phenoxy]-6-(*N*-ethyl-*N*-phenylamino)-*s*-triazine [25], 2,4-bis(3-chlorocarbonyl-2-naphthyloxy)-6-(2-naphthylamino)-*s*-triazine [26], and 2,4-bis(6-chlorocarbonyl-2-naphthyloxy)-6-(4-methyl-1-piperazinyl)-*s*-triazine [27] possessing good thermal stability, which was dependent on the type and structure of polymer. In the present work, we have synthesized and characterized various homopolyamides based on 2,4-bis-(6-chlorocarbonyl-2-naphthyloxy)-6-(4-methyl-1-piperazinyl)-*s*-triazine (MPNCCT).

Results and discussion

During the present investigation homopolyamides have been synthesized from MPNCCT and various diamines (Table 1), and evaluated in light of various physicochemical properties such as yield, color, solubility, density, viscosity, temperature characteristics, activation energy of thermal decomposition, IR spectra, and NMR shift. The molecular weight of these polyamides was determined by using the Mark-Houwink equation and found in the range of 200,000–290,000 g/mol.

Yield and color

The yield of homopolyamides varies from 60 to 90% depending upon the reactivity of the diamine component. The highest yield (90%) was obtained for PADADPA, while the lowest for PADADPS (60%). Most of the polyamides are light red to black. The color of polyamides involving 4,4′-diaminobenzanilide, 4,4′-diaminodiphenyl sulfone, 2,4-diaminotoluene, *m*-phenylenediamine, and *p*-phenylenediamine is darker than that of the other polyamides. All homopolyamides were obtained as solid powder. The yield and color of the polyamides depend upon the color, nature, and structure of the diamine components. The yield data of homopolyamides is presented in Table 2.

Density measurements

Density of each of the ten homopolyamides was determined at 25 ± 1 °C by the suspension method. The liquid system of carbon tetrachloride and petroleum ether was found to be inert to all homopolyamides. The sample remains in a state of suspension even after a long time. The results are shown in Table 2. Density of all homopolyamides varies from 1.216 to 1.087 g/cm^3. The highest density is displayed by PADADPSA, while the lowest by PAEDA. The density of the homopolyamides varies with the different chemical properties of the diamines used. PADADPSA shows the highest density value due to the small bond angle of $-SO_2-$ (106°), which leads to a compact structure and hence the highest density value [28].

The density of the homopolyamides obtained from MPNCCT and various diamines decreases in the following order:

PADADPSA > PADADPS > PAOPDA > PAPPDA
　> PADAT > PAMPDA > PADADPM > PADADP
　> PADADPA > PAEDA.
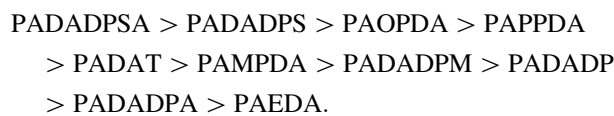
Solubility characteristics

Relative solubility of homopolyamides obtained from MPNCCT and various diamines in different solvents is presented in Table 3. Examination of the information presented therein reveals that polyamides derived from MPNCCT and various diamines are soluble in polar aprotic solvents like *N*-methyl-2-pyrrolidone (NMP), DMF, DMSO, *N,N*-dimethylacetamide (DMAc), *m*-cresol, sulfuric acid, and formic acid. The result for this may be that the presence of bulky side groups brings about an increase in solubility [29]. It is also found that the polyamides are insoluble in halogenated aliphatic and aromatic solvents

Table 1 Abbreviations and structures of homopolyamides

Diamine	Polymer	Structure
4,4′-Biphenyldiamine	PADADP	
4,4′-Diaminodiphenylmethane	PADADPM	
4,4′-Diaminodiphenyl sulfonamide	PADADPSA	
4,4′-Diaminodiphenyl sulfone	PADADPS	
4,4′-Diaminobenzanilide	PADADPA	

Table 1 continued

Diamine	Polymer	Structure
2,4-Diaminotoluene	PADAT	
p-Phenylenediamine	PAPPDA	
o-Phenylenediamine	PAOPDA	
m-Phenylenediamine	PAMPDA	
Ethylenediamine	PAEDA	

like chloroform, carbon tetrachloride, chlorobenzene, and bromobenzene. The polyamides are also insoluble in common organic solvents like benzene, cyclohexane, methanol, ethanol, acetone, and tetrahydrofuran. It is also observed that the solubility of the polyamides increases with an increase in temperature. The polymers, which are partly soluble at room temperature, get soluble at higher temperature (50 °C).

Table 2 Density and yield of homopolyamides

Polymer	Yield (%)	Density (g/cm^3)
PADADPS	90	1.205
PADADPSA	75	1.216
PADADP	70	1.155
PADADPA	60	1.151
PADADPM	65	1.159

Viscosity measurements

Dilute solution viscosity measurements were carried out using an Ubbelohde suspended level kinematic viscometer. Intrinsic, reduced, and inherent viscosities for all polyamides at various concentrations were determined at 25 ± 0.1 °C. The relative (η_{rel}) and specific (η_{sp}) viscosities were calculated. Reduced (η_{sp}/c) and inherent viscosities were then calculated from experimental data. Typical Huggins and Kraemer plots were used to obtain the intrinsic viscosity for each of the homopolyamides. Solution viscosity of PADADP at different concentrations is shown in Table 4. Intrinsic viscosity values for all polyamides are shown in Table 5. Intrinsic, reduced, and inherent viscosity along with Huggins and Kraemer constants for 1% solution for all polyamides reveals that PADADP has the highest solution viscosity and hence the highest molecular weight amongst the polyamides, whereas PAEDA has the lowest. Huggins and Kraemer plots for intrinsic viscosity are shown in Fig. 2.

Inherent viscosity values of polyamides were found higher than the inherent viscocity of corresponding copolyamides (except copolyamides from PA(DADPA + PPDA) [27]) and polyamides containing an *s*-triazine ring with thiophenoxy derivatives [21], and found nearly equivalent with polyamides containing fluorine "cardo" groups [23].

The intrinsic viscosity of the homopolyamides obtained from MPNCCT and various diamines follows the sequence given below:

Table 3 Solubility characteristics of homopolyamides

Solvent	PADADPA	PADADPSA	PADADPS	PADADPM	PADADP	PADAT	PAOPDA	PAMPDA	PAPPDA	PAEDA
H$_2$SO$_4$	++	++	++	++	++	++	++	++	++	++
m-Cresol	++	++	++	++	++	++	++	++	++	++
DMF	++	++	++	++	++	++	++	++	++	++
DMSO	++	++	++	++	++	++	++	++	++	++
DMAc	±+	++	++	±+	++	++	±+	++	++	±+
NMP	++	++	++	++	++	++	++	++	++	++
CHCl$_3$	− −	− −	− −	− −	− −	− −	− −	− −	− −	− −
THF	− −	− −	− −	− −	− −	− −	− −	− −	− −	− −
CH$_3$OH	− −	− −	− −	− −	− −	− −	− −	− −	− −	− −
CH$_3$CH$_2$OH	− −	− −	− −	− −	− −	− −	− −	− −	− −	− −
(CH$_3$)$_2$CO	− −	− −	− −	− −	− −	− −	− −	− −	− −	− −
C$_6$H$_6$	− −	− −	− −	− −	− −	− −	− −	− −	− −	− −

The first and second symbol indicate the solubility of a polymer at room temperature and 50 °C, respectively

"+" soluble, "−" insoluble, "±" partly soluble

Partly solubility for PADADPA $\approx$ 33% (w/v); PADADPM $\approx$ 30% (w/v); PAOPDA $\approx$ 35% (w/v); PAEDA $\approx$ 27% (w/v)

Table 4 Solution viscosity of PADADP

Conc. (g/dm^3)	Flow time t (s)	$\eta_{rel} = t/t_o$	$\eta_{sp} = \eta_{rel} - 1$	η_{sp}/c (dm^3/g)	ln η_{rel}/c (ln (dm^3/g))
2.0	149.3	1.176	0.176	0.088	0.081
4.0	174.5	1.374	0.374	0.093	0.079
6.0	202.0	1.590	0.590	0.098	0.077
8.0	232.0	1.827	0.827	0.103	0.075
10.0	264.5	2.083	1.083	0.108	0.073

Solvent: DMF, $t_o = 127$ s

Table 5 Various viscosity values of homopolyamides and constants of the Huggins and Kraemer equations

Polyamide	Intrinsic viscosity η	Reduced viscosity η_{sp}/c (dm^3/g)	Inherent viscosity ln η_{rel}/c (ln(dm^3/g))	Huggins constant K	Kraemer constant β
PADADP	0.831	0.108	0.073	0.364	0.140
PADADPM	0.817	0.106	0.072	0.376	0.135
PADADPSA	0.662	0.081	0.059	0.358	0.146
PADADPS	0.625	0.077	0.057	0.371	0.138
PADADPA	0.795	0.102	0.070	0.367	0.141
PADAT	0.711	0.088	0.062	0.317	0.168
PAPPDA	0.746	0.095	0.066	0.372	0.138
PAOPDA	0.723	0.090	0.064	0.356	0.147
PAMPDA	0.733	0.092	0.065	0.350	0.149
PAEDA	0.589	0.071	0.053	0.354	0.147

Concentration for all polymer solutions is 10 g/dm^3
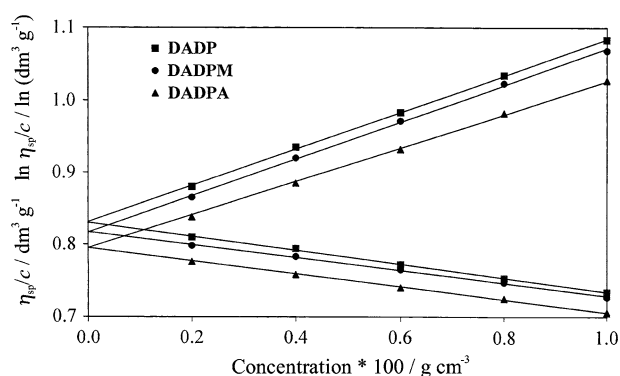
Fig. 2 Typical Huggins and Kraemer plots of intrinsic viscosity for PADADP, PADADPM, and PADADPA

PADADP > PADADPM > PADADPA > PAPPDA
   > PAMPDA > PAOPDA > PADAT > PADADPSA
   > PADADPS > PAEDA.

Infrared spectroscopy

The structure of the monomer employed for polyamide synthesis is such that all ten polyamides formed will be linear. The position of all easily discernible bands as well as of inflections at certain characteristic positions were noted and discussed.

The IR spectra of all polyamides exhibited a characteristic absorption band for N–H stretching at 3,250–3,350 cm^{-1}, which is due to the secondary amide character of the polyamides. The bands at 3,050–3,100 cm^{-1} are attributed to aromatic C–H stretching [30, 31]. Bands at 2,790–2,810 cm^{-1} are attributed to C–H-stretching vibration of –N–CH$_3$. The bands observed at 2,850–2,860 cm^{-1} and 2,920–2,930 cm^{-1} are assigned as symmetric and asymmetric C–H stretching vibrations of the –CH$_2$– group, respectively.
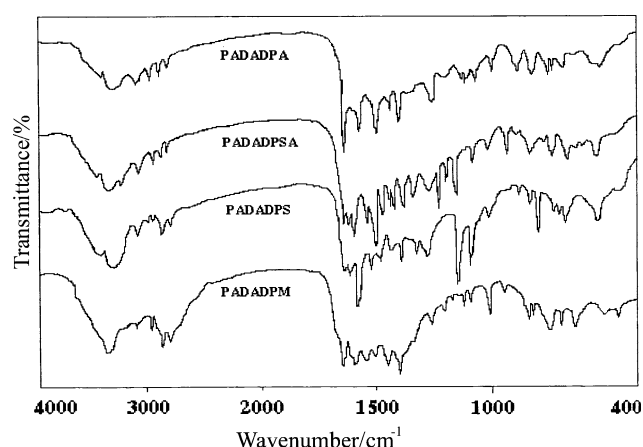
Fig. 3 IR spectra of PADADPA, PADADPSA, PADADPS, and PADADPM

The presence of amide carbonyl groups is indicated by a strong band in the region of 1,640–1,670 cm^{-1} (amide-I band). The band at 1,540–1,560 cm^{-1} is attributed to N–H bending vibration (amide-II band) [32]. The strong band in the region 1,400–1,500 cm^{-1} is attributed to skeletal ring stretching vibrations of aromatic and heteroaromatic rings. The strong band observed around 1,450–1,510 cm^{-1} is due to in-plane vibration of the *s*-triazine ring. The band in the region 1,380–1,400 cm^{-1} is attributed to C–N stretching vibrations of amide groups. The bands appearing at 1,020 cm^{-1} and 1,230–1,300 cm^{-1} are attributed to symmetric and asymmetric vibrations of the aryl-ether bond. In the spectrum of PADADPSA bands are observed around at 1,180 and 1,390 cm^{-1}, attributed to symmetric and asymmetric stretching vibration of the –SO$_2$NH– group. In the spectrum of PADADPSA and PADADPS, bands observed at 1,150 cm^{-1} and 1,320–1,340 cm^{-1} are attributed to stretching vibration of –SO$_2$– bond. The spectra of all
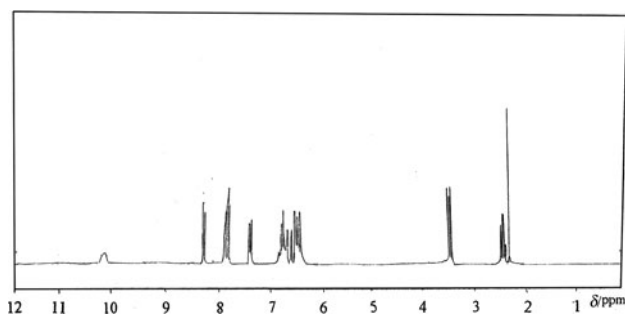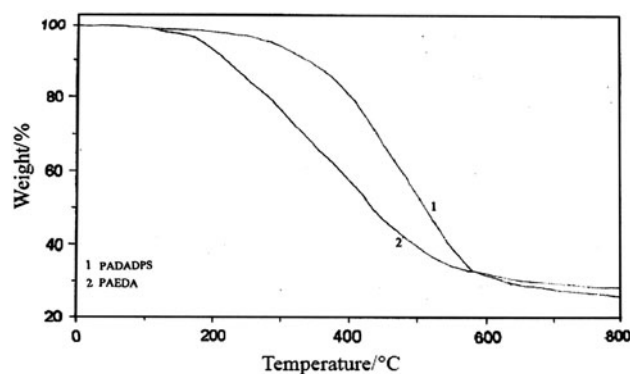
Fig. 4 NMR spectrum of PADADP

Fig. 5 Thermogram of PADADPS and PAEDA

Table 6 Temperature characteristics of polyamides (°C)

Polymer	T_0	T_{10}	T_{max}	T_s
PADADPS	285	330	435	515
PADADPA	280	300	350	390
PADAT	210	285	370	440
PAEDA	180	230	250	420

polyamide samples exhibited several common characteristic adsorption frequencies in the region 800–840 cm^{-1}, which are attributed to out-of-plane vibration of the s-triazine ring. In the spectra of PAOPDA, PAMPDA, and PAPPDA, bands observed around 780, 800, and 650 cm^{-1} may be attributed to the vibration of the o-, m-, and p-disubstituted phenyl ring, respectively. The band observed at 1,350 cm^{-1} in PADAT is attributed to the symmetrical bending vibration of the –CH$_3$ group [33]. Figure 3 shows IR spectra of PADADPA, PADADPSA, PADADPS, and PADADPM.

All above IR spectral characteristics of different polyamide samples are consistent with their proposed structures.

NMR spectroscopy

High-resolution (300 MHz) ^{1}H NMR spectra of the polyamide samples were consistent with their structure. The ^{1}H NMR spectrum of PAPPDA shows a multiplet at $\delta = 6.70–8.80$ ppm due to the presence of aromatic protons, a singlet at 2.35 ppm for the –N–CH$_3$ of the piperazine ring, a multiplet at $\delta = 2.50–3.70$ ppm due to the piperazine methylene groups, and a singlet at 10.20 ppm for –CONH– (Fig. 4).

The ^{1}H NMR spectrum of PADADP shows a multiplet at $\delta = 6.50–8.20$ ppm due to the presence of aromatic protons, a singlet at 2.25 ppm for the –N–CH$_3$ of the piperazine ring, a multiplet at $\delta = 2.50–3.60$ ppm due to the piperazine methylene groups, and a singlet at 10.10 ppm for –CONH–.

Thermogravimetric analysis

Stability at higher temperature is required for the polymers to be useful for special applications such as high-speed aircraft and missiles. In order to identify the general mechanism of decomposition of purified polymers in form of finely divided powder, thermal decomposition is carried out under inert atmosphere. Thermogravimetric curves obtained at a heating rate of 10 °C/min in nitrogen atmosphere (30 cm^3/min) for homopolyamides are shown in Fig. 5.

Qualitative estimation of thermal stability

Thermograms of all four polyamides exhibit single step thermal degradation. The relative thermal stability of polymers can be assessed by comparing the initial decomposition temperature (T_0), temperature for 10% weight loss (T_{10}), temperature for maximum rate of decomposition (T_{max}), and half volatilization temperature (T_s) in nitrogen atmosphere, as presented in Table 6.

The thermal stability of the homopolyamides on the basis of 10% decomposition temperature T_{10} is as follows:

PADADPS > PADADPA > PADAT > PAEDA

The thermal stability behaviour for maximum decomposition temperature is as follows:

PADADPS > PADAT > PADADPA > PAEDA

The thermogram of PADADPA reveals that the decomposition step begins at 285 °C. The decomposition is marked with a rapid weight loss in the temperature range 360–570 °C with the maximum rate of weight loss at 435 °C. The sample degrades slowly after 600 °C up to the end temperature and leaves about 26% residue.

The thermogram of homopolyamide of DADPA shows a single step of thermal degradation. The polymer begins to decompose at 280 °C. The maximum rate of weight loss occurs at 350 °C, involving about 35% weight loss. The residue left is about 28%.

Table 7 Application of the Broido method to the thermogram of PADADPS

T (°C)	% wt.	$y = \frac{W_t - W_\infty}{W_t - W_0}$	$1/y$	$\ln[\ln(1/y)]$	T (K)	$1/T \times 10^3$ (K^{-1})
405	78.25	0.7160	1.397	−1.096	678	1.475
415	73.50	0.6509	1.536	−0.846	688	1.453
425	72.00	0.6303	1.586	−0.774	698	1.432
435	70.00	0.6029	1.659	−0.681	703	1.422
445	69.00	0.5892	1.697	−0.637	713	1.402
455	67.50	0.5687	1.758	−0.572	723	1.383
465	63.50	0.5139	1.945	−0.408	733	1.364

Table 8 Application of Horowitz-Metzger's method to the thermogram of PADADPS

T (°C)	%wt	$1 - \alpha$	$1/(1 - \alpha)$	$\ln[\ln[1/(1 - \alpha)]]$	θ (°C)
405	78.25	0.7160	1.397	−1.096	−30
415	73.50	0.6509	1.536	−0.846	−20
425	72.00	0.6303	1.586	−0.774	−10
435	61.00	0.6029	1.659	−0.681	0
445	70.00	0.5892	1.697	−0.637	10
455	67.50	0.5687	1.758	−0.572	20
465	62.00	0.5139	1.945	−0.408	30

For PADAT, the polymer begins to decompose at 210 °C and undergoes a rapid weight loss in the temperature range 300–450 °C, involving 60% weight loss, with the maximum rate of weight loss occurring at 370 °C. After 550 °C, the sample degrades slowly up to the end temperature and leaves about 30% residue.

For PAEDA, the polymer begins to decompose at 180 °C. The decomposition is marked with a rapid weight loss in the temperature range 250–450 °C, involving 50% weight loss, with the maximum rate of weight loss occurring at 350 °C. After 500 °C, the sample degrades slowly up to the end temperature and leaves about 30% residue.

The thermal stability based on half volatilization temperature (T_s) follows a somewhat different sequence:

PADADPS > PADAT > PAEDA > PADADPA

The observation of above thermal stability trends shows that the homopolyamide of DADPS possesses the highest thermal stability while the homopolyamide of EDA possesses the least thermal stability.

Table 6 reveals that homopolyamides show higher thermal stability than corresponding copolyamides [27] but comparatively lower than polyamides containing an *s*-triazine ring with thiophenoxy derivatives [21] and polyamides containing fluorine "cardo" groups [23].
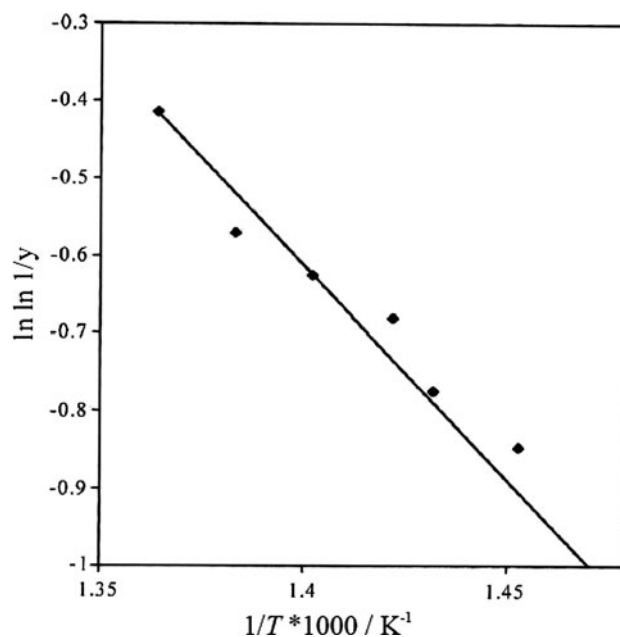
Fig. 6 Broido plot for PADADPS
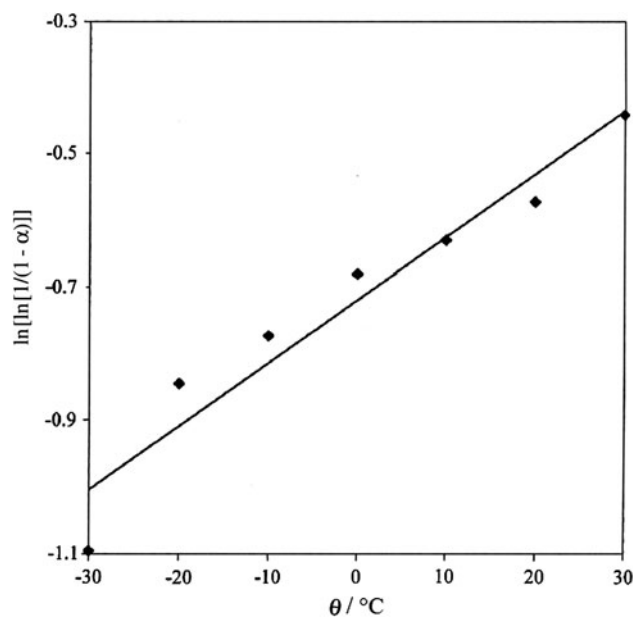
Fig. 7 Horowitz–Metzger plot for PADADPS

Evaluation of kinetic parameters

Dynamic TGA thermograms obtained at a heating rate of 10 °C/min have been analyzed by graphical methods proposed by Broido and Horowitz-Metzger. A typical application of the Broido method and the Horowitz-Metzger method is exemplified for PADADPS in Tables 7, 8, respectively, and relevant plots are shown in Figs. 6 and 7.

**Table 9** Kinetic parameters for the thermal decomposition of homopolyamides

Polyamide	Activation energy E (kJ/mol)	
	Broido	Horowitz-Metzger
PADADPS	45.64	40.83
PADADPA	81.50	82.42
PADAT	40.79	42.50
PAEDA	31.46	27.44

Since the magnitude of an apparent activation energy for degradation reaction reflects the ease with which it can proceed, it may be used to approximate the relative ease of thermal degradation of hompolyamides and hence, their relative thermal stability. The thermogram of PADADPS has been analyzed and described for activation energy using Broido and Horowitz-Metzger methods. Thermograms of other homopolyamides were also analyzed by the same graphical methods. The values of apparent activation energy corresponding to different decomposition steps involved are evaluated from the slope of the least square plots of the relevant data and are presented in Table 9. Examination of the data presented therein reveals that both methods result in comparable values for activation energy. The experimental points corresponding to initial stage (10% loss) of thermal degradation tended to deviate from linearity. This deviation may be due to the fact that the decomposition of solids does not obey first order kinetics in the initial stages. The Broido method is expected to provide comparatively reliable estimates of activation energy (E), since no other temperature characteristics are involved. The values of E vary from 31.46 to 81.50 kJ/mol according to the Broido method. The values of activation energy calculated according to the Horowitz-Metzger method are in good agreement with these values.

This trend of relative stability indicates that the initial site of degradation may lie in the nature of the bridge in the aromatic diamine component of the molecular chain. Thus, results based on qualitative and semiquantitative treatment of thermogravimetric data on polyamides point out that inclusion of the 4,4′-diaminodiphenyl sulfone moiety in a homopolyamide backbone is advantageous, so far as the thermal stability requirement is concerned.

Conclusion

A series of ten novel polyamides of high molecular weight was synthesized and characterized by solubility, density, viscosity, IR, NMR spectroscopy, and thermogravimetric
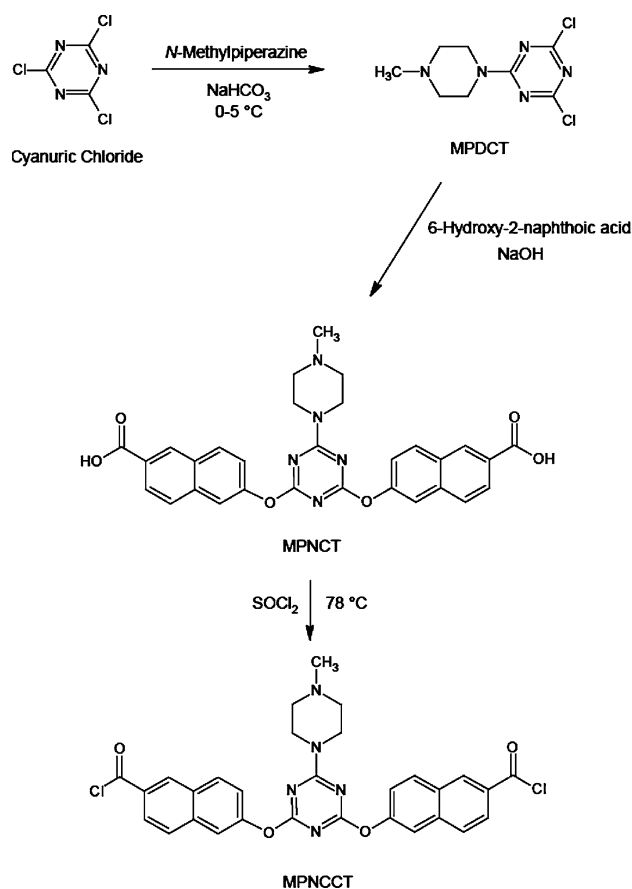
Fig. 8 Synthesis of the monomer 2,4-bis(6-chlorocarbonyl-2-naphthyloxy)-6-(4-methyl-1-piperazinyl)-s-triazine (MPNCCT)

analysis. These homopolyamides are found promising as materials of high thermal stability and processibility.

Experimental

Materials

Freshly prepared double distilled water was used for the preparation of solutions. Benzene, acetone, DMF, triethylamine, petroleum ether, carbon tetrachloride, methanol, ethanol, N-methyl-2-pyrrolidone, N,N-dimethylacetamide, dimethyl sulfoxide, m-cresol, sulfuric acid, and hexane were laboratory reagents and were used as received. Cyanuric chloride was purified by repeated crystallization from pure benzene (m.p. 146 °C). 4,4′-Diaminobenzanilide (DADPA) [34, 35] and 4,4′-diaminodiphenyl sulfonamide (DADPSA) [28] were synthesized by reported procedures. The other diamines such as 4,4′-diaminodiphenyl sulfone (Cibatul, Atul), 4,4′-diaminodiphenylmethane (Cibatul, Atul), 2,4-diaminotoluene (Merck), p-phenylenediamine (Merck), o-phenylenediamine (Merck), and ethylenediamine (Merck) of purity better than 99% were used as received.

Fig. 9 Synthesis of polyamide of 4,4′-diaminodiphenylmethane

MPNCCT + 4,4′-Diaminodiphenylmethane

Triethylamine | 160 ^{0}C

PADADPM
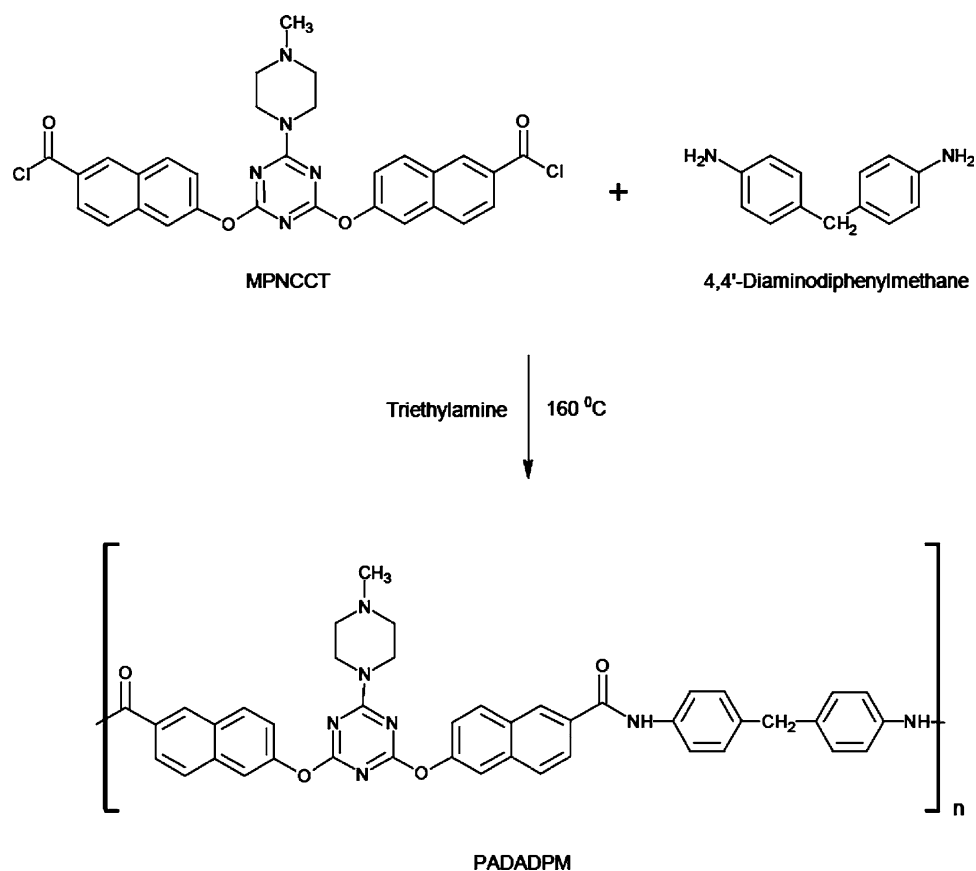
Techniques

Infrared spectra of all synthesized polymers have been measured using KBr pellets on a Perkin-Elmer FT-IR Spectrometer Paragon-500. NMR spectra of the polymers were recorded on a Perkin-Elmer Model-32 ^{1}H NMR Spectrometer (300 MHz) using DMSO-d_6 as solvent and TMS as reference compound. Density of the polymers was determined pyknometrically at 25 °C using the suspension method. Intrinsic viscosity was obtained from the plot of reduced viscosity versus concentration and inherent viscosity versus concentration according to Huggins and Kraemer equations. Thermogravimetric analysis of the some of the polymers have been carried out on a thermo-balance METTLER TA4000 system with constant heating rate of 10 °C/min in the temperature range from ambient to 800 °C. All thermograms were analysed by the graphical methods proposed by Broido and Horowitz and Metzger.

Synthesis of the monomer (MPNCCT)

The monomer, 2,4-bis(6-chlorocarbonyl-2-naphthyloxy)-6-(4-methyl-1-piperazinyl)-s-triazine (MPNCCT), was synthesized by the reaction described in Ref. [27] (Fig. 8).

Synthesis of polymers

A method for synthesis of polyamides from MPNCCT and 4,4′-diaminodiphenylmethane using the high temperature solution polycondensation technique is described as a model reaction.

Polyamide of 4,4′-diaminodiphenylmethane (PADADPM)

A mixture of MPNCCT (5.88 g, 0.01 mol), 4,4′-diaminodiphenylmethane (1.98 g, 0.01 mol), triethylamine (~5 cm^3), and minimum quantity of DMF (~10 cm^3) was placed in a three-necked flask equipped with a mechanical stirrer and a drying tube. The reaction mixture was heated with stirring at 165 °C for 8 h. At the initial stage of the reaction, the evolution of hydrogen chloride gas was rapid and later on slowed down. The polymer obtained was filtered, thoroughly washed with hot distilled water, then with hot methanol and hot acetone. Finally the polymer was dried in a vacuum oven at 80 °C over night. The yield of polymer was 80%.

The other polyamides from MPNCCT and various diamines such as 4,4′-biphenyldiamine (DADP), 4,4′-diaminobenzanilide (DADPA), 4,4′-diaminodiphenyl sulfone (DADPS), 4,4′-diaminodiphenyl sulfonamide (DADPSA), 2,4-diaminotoluene (DAT), o-phenylenediamine (OPDA),

m-phenylenediamine (MPDA), *p*-phenylenediamine (PPDA), and ethylenediamine (EDA) were synthesized by employing the same procedure and the similar reaction conditions as shown in Fig. 8. The structures of all polyamides are summarized in Table 1 (Fig. 9).

References

1. Yu G, Liu C, Zhou H, Wang J, Lin E, Jian X (2009) Polymer 50:4520
2. Kang WB, Sugiama T, Ogura S, Takano Y (1997) US Pat 5652327
3. Mahapatra SS, Karak N (2007) Polym Deg Stab 92:947
4. Shibasaki Y, Horie R, Takahashi T, Ichimura Y (1996) Thermochim Acta 282:530
5. Matsuo SJ (1994) Poly Sci Poly Chem 32:2093
6. Carothers WH, Berchet GJ (1930) J Am Chem Soc 52:5289
7. Carothers WH, Hill JW (1932) J Am Chem Soc 54:1566
8. Carothers WH (1937) US Pat 2071250
9. Carothers WH (1938) US Pat 2130947
10. Behniafar H, Khosravi-Borna S (2009) Polym Int 58:1299
11. Mallakpour S, Kolahdoozan M (2008) React Funct Polym 68:91
12. Han IS, Lee JY, Lee SI, Lee CB, Kwon SY (2009) US Pat 0253890A1
13. Fan SC, Li CL, Wang YC, Lee KR, Liaw DJ, Lai JY (2002) Desalination 148:43
14. Stevens MP (1990) Polymer chemistry: an introduction. Oxford, New York
15. Sweeney W, Zimmerman J (1961) Encycl Polym Sci Technol 10:483
16. Jacobs DB, Zimmeman J (1977) In: Schildknecht CE (ed) Polymerization process. Wiley, New York
17. Schule EC (1969) Encycl Polym Sci Technol 10:460
18. Teng MY, Lee KR, Liaw DJ, Lin YS, Lai JY (2000) Eur Polym J 36:663
19. Frazer AH (1968) High temperature resistant polymers. Wiley, New York
20. Rodriguez F (1996) Principles of polymer systems, 4th edn. Taylor and Francis, Washington
21. Pal RR, Patil PS, Salunkhe MM, Maldar NN, Wadgaonkar PP (2005) Polym Int 54:569
22. Sagar AD, Salunkhe MM, Wadgaonkar PP, Sarawade BD, Mahajan SS (1997) J Polym Sci Part A Polym Chem 35:1077
23. Sagar AD, Shingte RD, Wadgaonkar PP, Salunkhe MM (2001) Eur Polym J 37:1493
24. Patel HS, Patel KC (2006) Int J Polym Mat 55:1043
25. Patel HS, Patel KC (2006) Iran Polym J 15:505
26. Patel HS, Shah RR, Patel KC (2007) Int J Polym Mat 56:499
27. Patel KC, Asundaria ST, Patel PR (2010) Int J Polym Mat 59:118
28. Zhang S, Cheng X, Yang JZ (1999) Dyes Pigm 43:167
29. Slonimskii GL, Askadskii AA, Kitalgorodskii AT (1970) Polym Sci USSR 12:556
30. Whang WT, Wu SC (1988) J Polym Sci Polym Chem 26:2749
31. Herbenrother PM (1975) Macromol 7:575
32. Kim S, Pearce EM (1989) Makromol Chem 15:187
33. Philips JP, Merritt LL (1949) J Am Chem Soc 71:3984
34. Vogel AI (1989) Textbook of practical organic chemistry. Longman, London, p 1073
35. Simu GM, Chicu SA, Morin N, Schmidt W, Sisu E (2004) Turk J Chem 28:579